JOURNAL OF GEOPHYSICAL RESEARCH, VOL. 112, B03105, doi:10.1029/2006JB004340, 2007

Separation of paramagnetic and ferrimagnetic anisotropies: A review

Fátima Martín-Hernández[1] and Eric C. Ferré[2]

Received 10 February 2006; revised 7 November 2006; accepted 15 November 2006; published 28 March 2007.

[1] The magnetic anisotropy of rocks results from the contributions of diamagnetic, paramagnetic, and ferromagnetic (in the broad sense) minerals. This bulk anisotropy of magnetic susceptibility, which can be rapidly measured with modern instruments, generally provides a better understanding of the rock deformation history. Different minerals in a rock can form at different times and also respond to deformation in different manners. Therefore it is useful to separate their respective contributions to the whole rock magnetic fabric. Various techniques available to achieve this separation are presented and compared in this article. The variations of magnetic susceptibility with temperature can be used to selectively characterize the contribution of paramagnetic mineral phases following the Curie-Weiss law. The measurement of magnetic remanence-related anisotropy provides an efficient way to characterize the contribution of ferrimagnetic and antiferromagnetic species. Finally, measurement of the magnetic properties at high fields, above the saturation magnetization of ferromagnetic minerals, effectively separates the diamagnetic-paramagnetic magnetic anisotropy. The recent development of these techniques allows the separation of paramagnetic and ferrimagnetic anisotropies to be performed routinely on most specimens and shows promising potential for future magnetic anisotropy studies.

Citation: Martín-Hernández, F., and E. C. Ferré (2007), Separation of paramagnetic and ferrimagnetic anisotropies: A review, *J. Geophys. Res.*, *112*, B03105, doi:10.1029/2006JB004340.

1. Introduction to Magnetic Susceptibility and Its Anisotropy

[2] The magnetic susceptibility (K) is a dimensionless magnitude defined as

$$M = K H \tag{1}$$

where M is the induced magnetization and H is the applied field. In the International System [SI], magnetizations and magnetic fields are both measured in A/m; K is referred to as SI.

[3] In polymineralic rocks, the magnetic susceptibility is the sum of the magnetic susceptibilities of all rock-forming minerals. These may include diamagnetic, paramagnetic and/or ferromagnetic (in the broad sense) species. Figure 1 schematically shows the magnetic susceptibility of each type. Diamagnetic minerals do not have orbital moments in the absence of a magnetic field because all the orbitals are filled. Upon application of an external magnetic field, the angular momentum vector associated with the orbit precesses around the direction of the applied field and in the opposite direction. The induced magnetization disappears as soon as the magnetic field is removed The magnetic susceptibility is therefore negative and of small magnitude, typically on the order of -10^{-5} [SI] (Figure 1a). Paramagnetic materials have atoms with unpaired electron spins, oriented randomly in the absence of external fields. When a magnetic field is applied, a resultant moment arises in the direction of the field, and it disappears when the field is removed. The magnetic susceptibility is positive and typically on the order of 10^{-5} to 10^{-3} [SI], i.e., higher in absolute value than in diamagnetic minerals (Figure 1b). Ferromagnetic materials have uncompensated spins. The interaction of the uncompensated electron orbital give rise to an extra term of magnetic energy called the exchange energy. Ferromagnetic minerals can be subdivided into different types, such as ferromagnetic, ferrimagnetic, antiferromagnetic and spin-canted antiferromagnetic, depending on the configuration of the magnetic sublattices. As a consequence, a net magnetization appears in the absence of external fields. Magnetization is not a linear function with field (Figure 1c), and these minerals display an hysteresis loop of the magnetization as a function of the field [e.g., *Dunlop and Özdemir*, 1997].

[4] In most rocks the magnetic susceptibility is anisotropic, i.e., it varies with the direction of the applied field. This is caused by a combination of the preferred orientation of grains, the mineral grain spatial distribution or their lattice-preferred orientation, and the intrinsic anisotropy of the grains (shape or crystalline anisotropy). Another poten-

[1]Paleomagnetic Laboratory Fort Hoofddijk, Faculty of Geosciences, Utrecht University, Utrecht, Netherlands.
[2]Department of Geology, Southern Illinois University, Carbondale, Illinois, USA.

0148-0227/07/2006JB004340$09.00

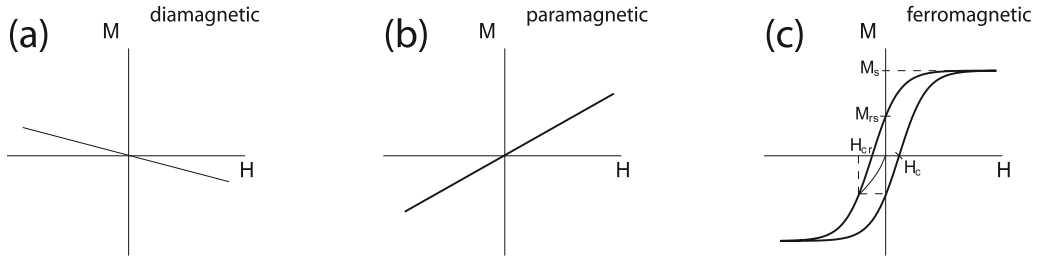

Figure 1. Schematic behavior of the magnetic susceptibility of three types of magnetic material: (a) diamagnetic, (b) paramagnetic, and (c) ferromagnetic.

tial source of anisotropy is distribution anisotropy or textural anisotropy, which occurs when ferromagnetic grains are close to each other in specific configurations [*Hargraves et al.*, 1991; *Stephenson*, 1994]. The anisotropy of magnetic susceptibility (AMS) is usually approximated by a symmetric second rank tensor, which can be represented as an ellipsoid with three principal axes ($K_1 \geq K_2 \geq K_3$) and their spatial orientation. In tensorial notation, equation (1) can be written as follows:

$$M_i = K_{ij}H_j \tag{2}$$

where M_i is the magnetization vector, K_{ij} is the susceptibility matrix, and H_j is the applied field vector.

[5] The anisotropy tensor is therefore represented by giving the orientation of the principal axes of the AMS ellipsoid and two scalars given the degree of anisotropy and shape of the ellipsoid. The degree of anisotropy of the ellipsoid can be described by several parameters, e.g., the ratio between the lengths of the maximum and minimum axes [*Nagata*, 1961] or the corrected anisotropy degree P' [*Jelinek*, 1981]. $P' = \exp\sqrt{2\Sigma(\ln K_i - \ln K)^2}$ (i = 1 to 3, K is the arithmetic mean susceptibility). P' is a measure of the degree to which the AMS ellipsoid deviates from a sphere. The shape of the AMS ellipsoid can vary from oblate, or disk-shaped, to prolate, or rod-shaped. Several approaches have been proposed to describe the ellipsoid shape such as the Flinn diagram [*Flinn*, 1956], the q parameter [*Granar*, 1958], the V parameter [*Graham*, 1954] or the T parameter [*Jelinek*, 1981]. $T = [(2 \ln K_2 - \ln K_1 - \ln K_3)/(\ln K_1 - \ln K_3)]$. The magnetic ellipsoid is oblate (pancake shaped) for $0 \leq T \leq 1$ and prolate (pencil shaped) for $-1 \leq T \leq 0$. The most common representation is the Jelìnek plot that shows the corrected degree of anisotropy (P') versus the T shape parameter. Figure 2a shows an example of the principal directions of the AMS ellipsoid in the Luarca Slates in the Asturian Arc, Northern Spain. The AMS ellipsoid shows well-grouped principal directions. Figure 2b shows an example of the Jelìnek plot in black slates from the Luarca Slates.

[6] The AMS was originally proposed by *Graham* [1954] as a useful fabric element. It has since become widely used in deformation studies because the AMS ellipsoid often correlates with the strain ellipsoid [e.g., *Hrouda et al.*, 1988; *Rochette et al.*, 1992; *Borradaile and Henry*, 1997]. The measurement procedures to determined the AMS ellipsoid are described by *Collinson et al.* [1967] and *Tarling and Hrouda* [1993].The contribution of each mineral species to the AMS of the rock depends on the mineral abundance, on the orientation of the grains (shape fabric) and also on the intrinsic magnetic anisotropy of the mineral grains. Minerals may form at different stages of a

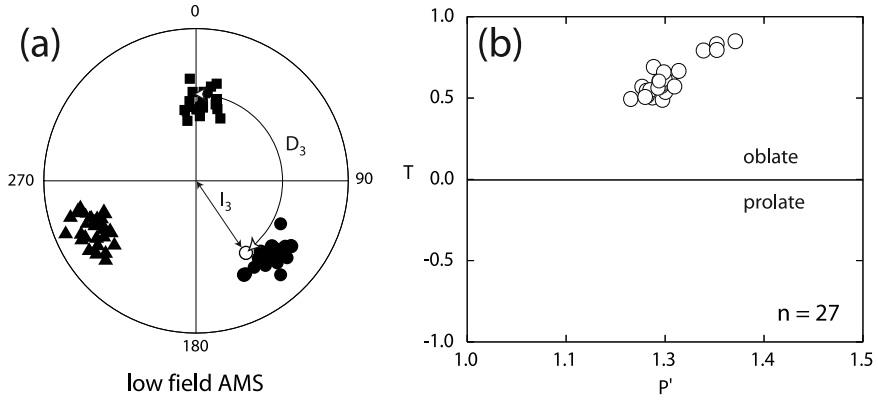

Figure 2. Most common representation of the principal directions of the AMS ellipsoid and its shape and degree of anisotropy on black slates from the Luarca Slates. (a) Lower hemisphere equal area projection of the AMS ellipsoid principal semiaxes where squares denote maximum susceptibility semiaxes, triangles denote intermediate susceptibility semiaxes, and circles denote minimum susceptibility semiaxes. The open symbol exemplifies the declination and inclination of one point. (b) Jelìnek plot displaying in the horizontal axes the degree of anisotropy (P') and in the vertical axes the shape parameter T [*Jelinek*, 1981].

Table 1. Summary of the Discussed Magnetic Anisotropy Techniques, Physical Property Measured, Advantages, and Disadvantages

Method	Magnitude Measured	Equipment	Advantages	Inconveniences
Low-field AMS	low-field magnetic susceptibility	AMS susceptibility bridge	fast; widely available	measures the resulting anisotropy of all the minerals present in the sample
Measurements at different temperatures				
Low-temperature methods	low-field magnetic susceptibility	AMS susceptibility bridge, liquid nitrogen	nondestructive	not possible for direct comparison of shape and degree of anisotropy with room temperature AMS; time intensive; increases the instrumental drift
High-temperature methods	low-field magnetic susceptibility	AMS susceptibility bridge, Furnace	masked fabrics can be revealed	not reversible; purely experimental, in some cases the enhanced fabric is more random; produces mineral changes
Measurements of magnetic remanence				
Anisotropy of Anhysteretic Remanence	anhysteretic remanence magnetization	magnetometer, AF coil and DF coil or Helmholtz cage	discriminates coercivity fractions; not affected by inverse fabric	time intensive; problems with saturation on hematite/pyrrhotite; not comparable with AMS
Anisotropy of Isothermal Remanence	isothermal remanence magnetization	magnetometer, HF permanent magnet or pulse magnetizer	possibility to isolate the anisotropy of hematite alone	spurious magnetizations and magnetic memories; not applicable in the Rayleigh region
Gyroremanence and rotational remanence	gyroremanence magnetization	magnetometer, AF coil	isolates magnetic fabrics of specific minerals (e.g., greigite)	time consuming; only valid with some magnetic minerals
Measurements in high-field				
High-field Torque Magnetometer	magnetic torque	high-field torque magnetometer	separates paramagnetic, ferromagnetic and antiferromagnetic components; provides other rock magnetic; parameters such as rotation hysteresis loss	deviatoric tensor only; time intensive; not widely available
HF-cryogenic magnetometer	remanent magnetization in high-field at low temperature	cryogenic magnetometer	separates paramagnetic, ferromagnetic and antiferromagnetic components; provides the full susceptibility tensor	size limitations; not suitable for very strongly magnetic samples; not available
Vibrating sample magnetometer	in-field magnetization	vibrating sample magnetometer (VSM)	very fast; nondestructive	problems with hematite/goethite; sample size
Other methods				
Using frequency dependency	low-field magnetic susceptibility	AMS susceptibility bridge operating at different frequencies	identification of minerals such as pyrrhotite; reversible; fast; nondestructive	computes the anisotropy of all the minerals at different frequencies, does not separate subfabrics; not available; theoretical method not developed
Statistical	low-field magnetic susceptibility	AMS susceptibility bridge	can be applied to one particular site independently of other experiments; can remove tectonic overprints	only work with homogeneous deformations; requires large number of samples

rock's deformation history, and therefore their magnetic fabrics may record different deformation events. For example, alteration minerals may form late, and their magnetic fabric may be geometrically unrelated to the previous deformation history.

2. Rationale for Separation of Magnetic Anisotropies

[7] The separation of the magnetic susceptibility only (scalar) into paramagnetic and ferromagnetic components does not require oriented specimens and can be performed on small volumes of material (≈ a few mm3). In contrast, the separation of the AMS into paramagnetic and ferromagnetic directional components involves measurements in different directions on oriented specimens and generally requires larger volumes to be analyzed (≈ a few cm3; although a successful separation was performed by *Borradaile and Werner* [1994] on millimeter size single crystals, using an alternating gradient magnetometer). One of the first reported separations of ferromagnetic and paramagnetic susceptibility anisotropies concerned a single crystal of augite hosting maghemite inclusions [*Owens and Bamford*, 1976]. Since this original work, several separation methods have been proposed using the variation of susceptibility with either temperature or applied field. Separation methods can be further subdivided into those based on tensor subtraction and those based on instrumental isolation of one of the magnetic anisotropy components (usually the paramagnetic AMS). Major progress has been made in the last few years, both from a theoretical and experimental point of view, in the separation of magnetic anisotropy into its components. Table 1 summarizes the current techniques, instrumental requirements, physical property measured, advantages and disadvantages compared to standard low-field AMS measurements.

[8] The need to isolate the contribution of each mineral to the total magnetic anisotropy was recognized early by *Owens and Bamford* [1976] and later on by *Rochette and Fillion* [1988]. The distinction of diamagnetic, paramagnetic and ferromagnetic anisotropies has been previously discussed by *Tarling and Hrouda* [1993].

[9] The main motivation for the separation results from the possibility of using the magnetic fabric as a proxy for bulk mineral fabric. Classic fabric techniques such as the universal stage, electron backscatter diffraction, texture goniometry, neutron diffraction or image analysis are time consuming, typically on the order of several hours per specimen. The measurement of magnetic fabrics is, in contrast, rapid and highly reproducible. Another difficulty with classic fabric techniques is the relatively small volume being measured (usually a thin section, ≈40 mm3) compared to that measured in magnetic techniques (≈8 to 10 cm^3). For these reasons, classic fabric techniques are more dependent on the grain size of rocks than magnetic techniques and are less representative of the rock fabric.

[10] For example, the olivine lattice preferred orientation of a coarse-grained peridotite may appear more strongly oriented than that of a fine-grained peridotite simply because fewer grains would have been measured in the coarse-grained rock [*Newman et al.*, 1999]. *Lüneburg et al.* [1999] showed that the mineral fabric observed in SEM photomicrographs of slates did not correspond with the finite strain measured by macroscopic strain makers such as micropebbles and reduction spots. However, the finite strain principal semiaxes correlated well with the AMS principal eigenvalues.

[11] Mineral fabrics are particularly valuable to determine paleocurrent direction or burial compaction in sediments, flow direction in igneous rocks and deformation history of rocks [*Kodama*, 1995]. Nevertheless, before magnetic fabrics can be interpreted as a proxy for mineral fabrics, it is necessary to identify the mineralogical sources of magnetic anisotropy. This is particularly important in the case of low anisotropies because even a small quantity of weakly oriented but strongly ferromagnetic minerals can overshadow the fabric of paramagnetic minerals [e.g., *Borradaile and Werner*, 1994]. The contribution of each mineral phase to the magnetic susceptibility does not necessarily correlate with its contribution to the anisotropy of magnetic susceptibility (AMS).

[12] A number of specific reasons for the separation of magnetic contributions to the anisotropy have been identified:

[13] 1. In paramagnetic single-crystal studies, inclusions commonly consist of ferrimagnetic minerals, which affects the geometric relationship between crystallographic fabric and AMS axes [e.g., *Owens and Bamford*, 1976; *Zapletal*, 1990; *Borradaile and Werner*, 1994; *Lagroix and Borradaile*, 2000; *Martín-Hernández and Hirt*, 2003].

[14] 2. Ferromagnetic (in the broad sense) minerals may be secondary in origin, in which case their fabric would relate only to the late stages of deformation; typically, this would occur as a result of oxidation of primary ferromagnetic minerals (magnetite ↔ hematite) [*Just et al.*, 2004] or as a result of thermal alteration due to burial of iron oxides (goethite ↔ hematite) [*Sangode and Bloemendal*, 2004]. In hydrothermal systems, goethite can carry an antiferromagnetic anisotropy [*Sizaret et al.*, 2003].

[15] 3. The AMS of ferrimagnetic minerals is often used to remove postmagnetization deformation such as compaction and its effects (inclination shallowing) in paleomagnetic studies [*Jackson et al.*, 1991; *Kodama and Sun*, 1992]; the AMS of the paramagnetic matrix may reflect more accurately the finite strain ellipsoid; some models that have correlated AMS with finite strain use the degree of anisotropy as the correlation variable; however, the degree of anisotropy can increase because of a larger ferromagnetic content and not necessarily as a consequence of higher strain rates [e.g., *Rochette et al.*, 1992].

[16] 4. Paramagnetic minerals generally represent a larger volume fraction than ferromagnetic minerals in rocks and therefore are likely to yield more reliable fabric information.

[17] Ferromagnetic minerals potentially carry supplemental vorticity information in cases where both ferromagnetic and paramagnetic minerals are primary and have distinct aspect ratios (Figure 3) [e.g., *Ferré et al.*, 2004]. Ferromagnetic fabric is affected by domain state (inverse fabric [e.g., *Rochette*, 1988; *Ferré et al.*, 2002]), grain size [*Hejda et al.*, 1992] and interaction between particles [*Gregoire et al.*, 1995; *Cañón-Tapia*, 2001].

[18] In summary, the separation of the various contributions of diamagnetic, paramagnetic and ferromagnetic min-

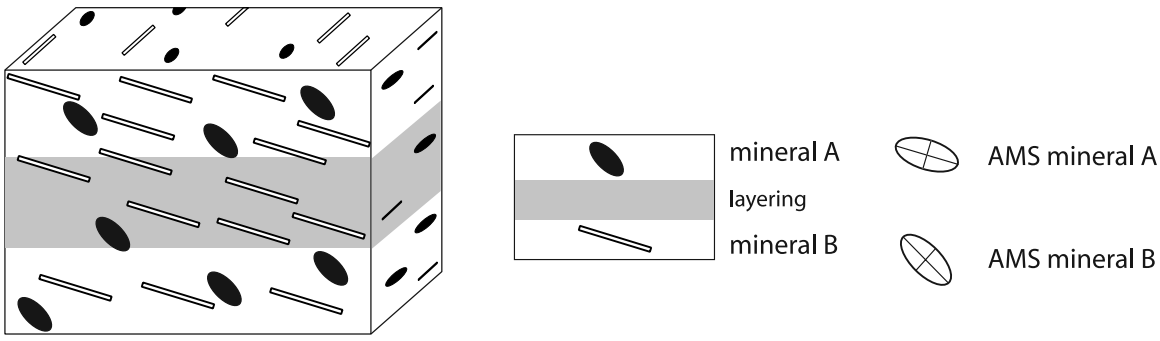

Figure 3. Schematic configuration for the AMS of ferromagnetic and paramagnetic minerals.

erals to the AMS has fundamental implications in strain analysis and has numerous applications in structural geology and paleomagnetism.

[19] In the current review, we briefly introduce the rationale for the separation, present and discuss the various approaches and finally elaborate on future methodological challenges. Unless otherwise specified, magnetic susceptibility refers to that measured in low field. The purpose of the paper is to provide a simple comparison of the variety of possible techniques of subfabric separation, which could be used on each study, their advantages and disadvantages (Table 1).

3. Methods Based on Measurements at Different Temperatures

3.1. Low-Temperature Methods

[20] The magnetic susceptibility K of a paramagnetic mineral increases with decreasing temperature according to the Curie-Weiss law [e.g., *Morrish*, 1965]:

$$K = \frac{C}{(T-\theta)} \tag{3}$$

with C the Curie constant of the mineral, T the temperature in Kelvin, and θ the paramagnetic Curie temperature in Kelvin. Equation (3) can also be expressed as

$$\frac{1}{K} = \frac{1}{C}(T-\theta) \tag{4}$$

Figure 4a exemplifies the relationship expressed in equation (4) in a biotite single crystal. Fitting the inverse of the susceptibility into a straight line, the paramagnetic Curie temperature is computed showing a positive value in the basal plane and negative value perpendicular to it. This result denotes the antiferromagnetic character of the interaction of cations along the crystal c axes [*Ballet and Coey*, 1982; *Beausoleil et al.*, 1983]. The variation is substantial since a temperature decrease from 295 to 77 K would result in an increase in magnetic susceptibility by a factor of ≈3.8. For diamagnetic minerals there is no change in magnetic susceptibility with temperature. In contrast, ferromagnetic minerals such as titanomagnetite and multidomain magnetite exhibit significant magnetic susceptibility changes below the Verwey transition [e.g., *Verwey*, 1939; *Dunlop and Özdemir*, 1997]. Hematites display a magnetization transition (Morin transition) at 242 K in which the spin orientation is changed from perpendicular to parallel to the c axis [*Morin*, 1950; *Liu*, 1986; *de Boer et al.*, 2001].

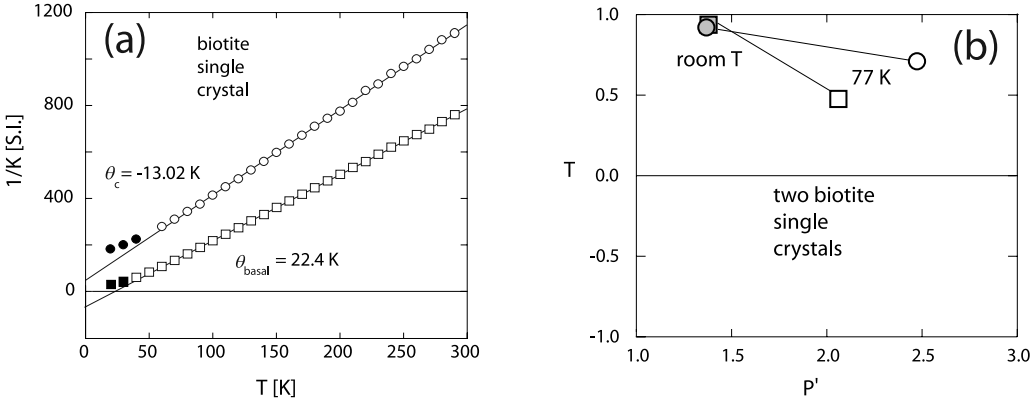

Figure 4. Variation of the magnetic susceptibility with temperature for paramagnetic minerals in biotite single crystals from Bancroft, Canada. (a) Inverse of the magnetic susceptibility as a function of temperature for a biotite single crystal measured in one direction within the crystal basal plane (open squares) and along the c axes (open circles). (b) Jelìnek plot for the anisotropy of magnetic susceptibility of two biotite single crystals measured at 77 K (open symbols) and compared with the AMS at room temperature for the same samples (solid symbols).

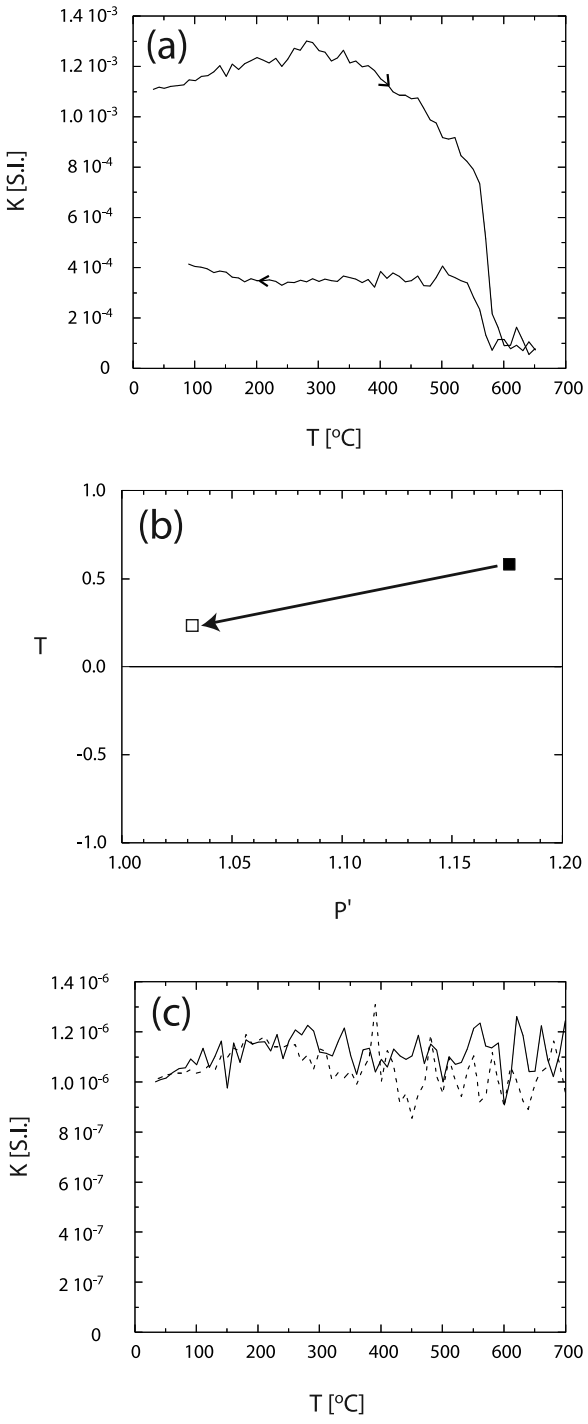

Figure 5. Magnetic susceptibility and AMS on a thermally enhanced dunite sample from the Twin Sisters massif, Washington State. (a) Thermomagnetic curve performed in a Sapphire Instrument SI-3. The arrows show the warming up and cooling down branches of the curve. (b) Jelìnek plot showing the variation of AMS parameters on one sample heated up to 700°C and cooled down again to room temperature. Solid symbol represents the unheated sample and open symbol the heated sample. (c) Magnetic susceptibility measured with the furnace empty. Solid line represents the warming up branch of the curve, and dotted line shows the cooling down branch.

[21] The variations of K at low temperature have been used to enhance and quantify the contribution of paramagnetic minerals to the bulk magnetic susceptibility [*Schultz-Krutisch and Heller*, 1985; *Jover et al.*, 1989; *Richter and van der Pluijm*, 1994] and to the AMS [*Ihmlé et al.*, 1989; *Hirt and Gehring*, 1991; *Richter and van der Pluijm*, 1994; *Lüneburg et al.*, 1999; *Parés and van der Pluijm*, 2002b]. In order to avoid temperature heterogeneity, specimens are measured in different directions while immersed in liquid nitrogen (77 K). This method, which does not induce any mineralogical changes in the analyzed material, allows to repeat measurements on the same specimen and enhances the degree of anisotropy (P') of paramagnetic phases [*Lüneburg et al.*, 1999; *Parés and van der Pluijm*, 2002a]. However, it also produces variations of the shape of the AMS ellipsoid, as shown in Figure 4b for two biotite crystals measured at different temperatures, making the interpretation of the low-T AMS results more complicated.

[22] The potential of low-temperature methods resides in the enhancement of the paramagnetic contribution to the bulk AMS. The separation of the AMS into its paramagnetic and ferromagnetic components involves subtracting the low-field AMS tensor from the low-temperature (LT) AMS tensor. This may lead to error amplification since low-temperature measurements enhance the error on susceptibility meters [*Parés and van der Pluijm*, 2002b]. Another potential difficulty arises from the large variations in magnetic susceptibility of ferromagnetic minerals at low temperature (Morin and Verwey transitions).

3.2. High-Temperature Methods

[23] With increasing temperature, the magnetic susceptibility (K) of diamagnetic minerals remains constant whereas that of paramagnetic minerals decreases according to the Curie-Weiss law (equations (3) and (4)). The magnetic susceptibility of ferromagnetic minerals (in the broad sense) displays more complex variations. In a field of strength similar to the Earth's field, the ferromagnetic susceptibility increases gradually with increasing temperature up to the Curie temperature (Tc) and then it decreases abruptly [e.g., *Stacey and Banerjee*, 1974; *Hrouda et al.*, 1997]. The increase in magnetic susceptibility below T_c, referred to as the Hopkinson effect, is less pronounced in high field [*Nagata*, 1961]. The Curie temperature varies with the composition of the ferromagnetic mineral. In the magnetite (Fe_3O_4)–ulvöspinel (Ti_3O_4) solid solution, for example, the Curie temperature decreases as the mole fraction of ulvöspinel (x) increases according to empirical formulas [*Uyeda*, 1958; *Schmidbauer and Readman*, 1982; *Clark and Evans*, 1997]. *Miranda et al.* [2002] proposed the following relationship: T_c (°C) = 575 − 552.7x − 213.3 × 2. The Curie temperatures of pure ferromagnetic minerals are 680°C for hematite, 580°C for magnetite and 320–330°C for pyrrhotite [e.g., *Dunlop and Özdemir*, 1997]. At such high temperatures, thermally induced reactions commonly take place, and therefore such experiments are typically nonreversible (Figure 5a). The creation of new magnetic phases leads to variation in the AMS parameters, shape and degree of anisotropy (Figure 5b). In order to improve the reversibility, experiments can be conducted under controlled atmosphere (Ar or N_2) to prevent oxidation or reduction of the original minerals.

[24] Thermally induced reactions have been used to enhance magnetic fabrics in weakly anisotropic rocks by forming new ferromagnetic minerals [*Hirt and Gehring*, 1991; *Hrouda et al.*, 1997; *Trindade et al.*, 2001b; *Mintsa Mi Guema et al.*, 2002]. In such experiments, magnetite is commonly formed upon heating. The grain size of the new magnetite crystals depends on the heating time but also on the original iron content of the material. The newly formed minerals do not necessarily grow mimetically to the original fabric [*Henry et al.*, 2003] and therefore this approach has substantial limitations. In principle, AMS measurement above T_c could remove the contribution of ferromagnetic minerals and therefore could isolate the diamagnetic-paramagnetic contribution to the AMS. However, experiments conducted on magnetite-bearing rocks at 640°C, using a Sapphire Instrument SI-3B furnace, suggest that background magnetic noise is too high to ensure sufficient sensitivity. Changes in temperature of the measuring coil induce dilation of the coil metal which is accommodated by creep along random segments of the coil. This in turn slightly modifies the coil geometry and causes important variations of the measured susceptibility. These large variations are shown on Figure 5c.

4. Methods Based on Measurement of Magnetic Remanence

[25] The anisotropy of magnetic remanence (AMR) evaluates the anisotropy of the minerals that are able to retain stable permanent magnetization. It does not provide a separation of AMS components but an independent estimate of the remanence anisotropy of ferromagnetic phases. In general, the magnetic remanence is carried mostly by the single-domain (SD) and pseudosingle-domain (PSD) ferromagnetic minerals (in the broad sense). The magnetization is, in first approximation, proportional to the applied field in weak fields:

$$\overline{M}_R = K_R \overline{H} \tag{5}$$

where $\overline{M}_R$ is the remanent magnetization, K_R is the susceptibility of remanence, i.e., the proportionality constant and $\overline{H}$ is the applied field.

[26] The susceptibility of remanence is commonly represented as a second rank tensor [e.g., *Jackson*, 1991]. Different types of remanence anisotropy can be measured depending on the nature of the applied field and type of acquired remanence. The two most common techniques to measure the anisotropy of remanent magnetization are the anhysteretic remanent magnetization (ARM) and the isothermal remanent magnetization (IRM). Both methods require artificial magnetizations acquired using techniques available in paleomagnetic laboratories [e.g., *Jackson and Tauxe*, 1991; *Rochette et al.*, 1992; *Tarling and Hrouda*, 1993; *Borradaile and Henry*, 1997]. The measurement procedure for the anisotropy of remanent magnetization is similar to that used in the determination of the low-field AMS. The number of orientations used for the determination varies from a minimum of 3 [*Potter and Stephenson*, 1990] up to 24 [*Trindade et al.*, 2001a]. The most common schemes are either 9 [*McCabe et al.*, 1985; *Borradaile and Stupavsky*, 1995] or 15 [*Cox and Doell*, 1967]. A comprehensive summary of techniques and uses of magnetic remanence anisotropy methods is given by *Potter* [2004].

4.1. Anisotropy of Anhysteretic Remanence

[27] The anisotropy of anhysteretic remanence (AARM) technique was first presented as a correlation between the anisotropy of this remanence type (anhysteretic remanence magnetization, ARM) and low-field AMS principal directions [*McCabe et al.*, 1985]. For the ARM, considering a weak field remanence, the magnetization is supposed to be linearly proportional to the applied field as described by equation (5). Samples are exposed to an alternating field (AF), on the order of 100 mT, and to a steady field, usually on the order of magnitude of the Earth magnetic field [see *Jackson*, 1991]. All magnetic particles with the coercivity of the chosen AF field are magnetized and their anisotropy computed by fitting the results to the best ellipsoid, usually by least squares methods [*Girdler*, 1961]. These techniques are commonly used in rock types such as pelites [*Debacker et al.*, 2004], granites [*Trindade et al.*, 2001a], limestones [*Hrouda et al.*, 2000] or basalts [*Borradaile and Lagroix*, 2001]. Figure 6 shows a comparison between the AMS measured at low field and the AARM of one peridotite sample from the Twin Sisters dunite, Washington [*Ferré et al.*, 2005]. The main ferromagnetic mineral, identified as magnetite, formed during moderate serpentinization [*Ferré et al.*, 2005]. In this example, the low-field K1 direction does not agree with the mineral lineation. Figure 6a shows how one of the maximum susceptibility semiaxes agrees well between the two methods, while the other two are dispersed over a great circle. Minimum and intermediate susceptibility semiaxes are not lying in a geologically meaningful plane. There is no direct comparison for the degree of anisotropy and shape between the AMS and the AARM ellipsoid (Figure 6b). The degree of anisotropy is usually larger for the AARM ellipsoid than for the AMS ellipsoid and the shape is more neutral in most of the reported cases [*Lagroix and Borradaile*, 2000].

[28] On the basis of the acquisition of ARM within a coercivity window, the most common technique of AARM is the partial AARM (pAARM) proposed by *Edwards* [1984] and *Jackson et al.* [1988]. The samples are placed in a decaying alternating field with no static field. At a given alternating field peak (H_1), the direct current (DC) field is switched on and then off again at a second alternating current field (H_2). The magnetic particles with coercivity between H_1 and H_2 are magnetized. By repeating the process in different orientations, the pAARM ellipsoid is computed for the specific coercivity window. The technique has been shown to be useful to discriminate differences in the anisotropy directions carried by different grain sizes or nature [*Nakamura and Borradaile*, 2001; *Aubourg and Robion*, 2002].

[29] The most used application of this technique is to correct inclination shallowing effects by calculating the AARM ellipsoid. The correction factor has been related with the ratio of the AARM semiaxes [*Jackson et al.*, 1991; *Collombat et al.*, 1993]. The relationship between inclination and AARM semiaxes is based on the following formula, although some variations have been proposed for each particular case.

$$\tan(I_c) = k \tan(I_{DRM}) \tag{6}$$

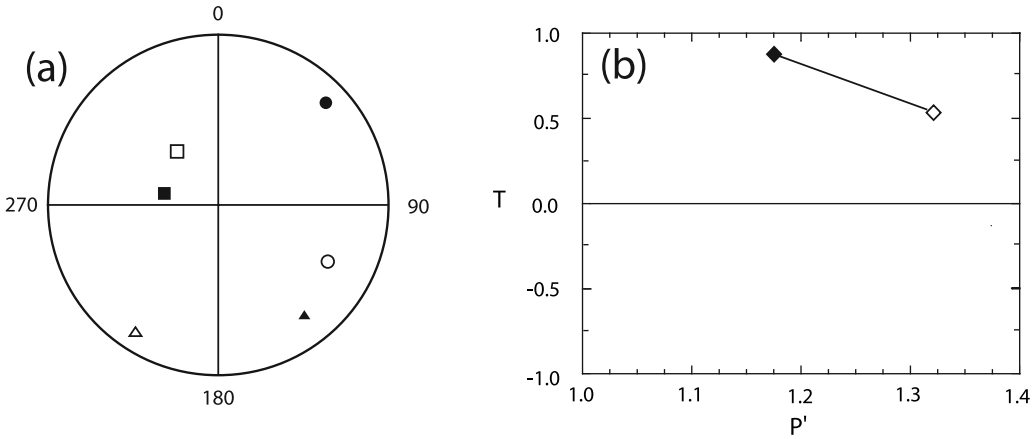

Figure 6. Comparison between the AMS and AARM for peridotite sample from the dunite Twin Sisters. The ARM for the AARM ellipsoid has been determined with a DC field of 100 mT. (a) Comparison between the low-field AMS ellipsoid principal directions (solid symbols) and the AARM ellipsoid principal directions (open symbols). (b) Jelinek plot with shape factor of the ellipsoid (T) versus the degree of anisotropy (P') for the low-field AMS (solid diamond) and the AARM (open diamond).

where I_c is the corrected inclination, k is the proportionality constant and I_{DRM} is the inclination of the detrital remanent magnetization.

[30] The constant k has been found to be proportional to the ratio of AARM semiaxes, such as the expressions proposed by *Jackson* [1991] and *Collombat et al.* [1993]:

$$k \propto \left(\frac{AARM_{\min}}{AARM_{\max}}\right)^n \tag{7}$$

where n is an exponent which is taken as 1 by *Jackson* [1991] and as 3 by *Collombat et al.* [1993]. This correction has been successfully used in the calculation of inclinations with a combination of AMS and pAARM or total AARM [*Hodych et al.*, 1999; *Kim and Kodama*, 2004; *Vaughn et al.*, 2005].

4.2. Anisotropy of Isothermal Remanence

[31] The use of the Isothermal Remanent Magnetization (IRM) as magnetization for the determination of the anisotropy of remanence was first proposed by *Daly and Zinsser* [1973]. It is based on the magnetization is proportional to the applied field relationship. The remanence of the IRM is measured and then removed by AF demagnetization on a peak field higher than the DC field, which ensures a perfect cleaning of the artificial magnetization. The applied DC field is usually in the range of 10–60 mT [*Stephenson et al.*, 1986; *Cagnoli and Tarling*, 1997; *Robion et al.*, 1999; *Raposo and Egydio-Silva*, 2001; *Hrouda*, 2002; *Raposo et al.*, 2004]. The DC field can also be applied in opposite directions successively. Therefore the remanence is measured twice and the residual of the imparted isothermal remanence is calculated by substraction [*Robion et al.*, 1999]. This procedure allows testing the presence of preferred directions in the remanence due to spurious magnetizations [*Tauxe et al.*, 1990]. The magnetization is removed with an AF demagnetization (cleaning) with maximum fields ranging from 80 to 100 mT.

[32] The validity of this method has been debated since its appearance. The IRM remanence is not linear with field and therefore the approximation given by equation (5) might not be valid. Three approaches have been proposed in order to determine the AIRM ellipsoid:

[33] 1. Very low IRM fields where the relationship given in equation (3) is still valid are in the order of 5–10 mT. The approximation is valid for magnetite-bearing rocks over a large range of grain sizes [*Stephenson et al.*, 1986].

[34] 2. Expand the relationship between magnetization and applied field into a nonlinear function. As first approximation, equation (3) can be expressed differently including a function f(H), containing the nonlinear relationship between the applied field and the magnetization [*Daly and Zinsser*, 1973; *Jelinek*, 1993; *Hrouda*, 2002]:

$$\mathbf{M}_r = \mathbf{K}_r f(H)\mathbf{e}_H \approx \mathbf{R}H^2\mathbf{e} \tag{8}$$

where M_r is the remanence magnetization, K_r is the remanence susceptibility matrix, f(H) is the nonlinear field dependency of the magnetization and $\mathbf{e}_H$ a unit vector in the direction of the applied field and $\mathbf{R}$ is the remanebility tensor of first kind [*Daly and Zinsser*, 1973; *Jelinek*, 1993].

[35] 3. Apply a saturating IRM field (SIRM) that resets the magnetic moment for every applied field direction. For magnetite-bearing rocks, this requirement can be met by applying a SIRM field of 300 mT [*Borradaile and Dehls*, 1993; *Lu and McCabe*, 1993]. The method is only applicable to low-coercivity specimens with no traces of high-coercivity minerals. Because hematite cannot saturate with the field available in most paleomagnetic laboratories, some authors have opted to apply high IRM fields in different directions where magnetization is more than 70% of the SIRM [*Tan and Kodama*, 2002; *Tan et al.*, 2003]. The method is under debate and it could be affected by the magnetization history of hematite [*Smith and Fuller*, 1967]. A real AIRM for hematite bearing rocks would require applying fields over 13 T to ensure the particles reach saturation for every measured direction [*Kodama and Dekkers*, 2004].

4.3. Other Remanence Anisotropy Methods

[36] Gyroremanent magnetization (GRM), another type of magnetization, is acquired by magnetic particles in an

alternating field even if no direct current field is present [*Stephenson*, 1980a, 1980b]. Some have suggested that it might be a source of spurious magnetization in alternating field demagnetization cleaning [*Dankers and Zijderveld*, 1981; *Roperch and Taylor*, 1986]. GRM has been satisfactorily modeled for SD anisotropic particles as due to the motion of the magnetic moment as it moves with the applied field direction [*Dean et al.*, 1990]. The anisotropy of GRM reflects the sample fabric in several types of natural samples [*Stephenson*, 1980b, 1981b] and artificial samples [*Stephenson*, 1981a; *Stephenson and Potter*, 1987; *Vincent et al.*, 1996]. Greigite displays a strong GRM acquisition and the anisotropy of GRM can be used to isolate its magnetic fabric of greigite-bearing samples [*Snowball*, 1997a, 1997b; *Hu et al.*, 1998; *Stephenson and Snowball*, 2001; *Hu et al.*, 2002].

[37] Rotational remanence (RR) is a particular type of gyroremanence magnetization recorded by magnetic particles when rotating them with their axis normal to an alternating field. The field should be approximately twice the frequency of the frequency of the rotation [*Stephenson*, 1980c]. The anisotropy of rotation remanence magnetization (ARRM) is particularly important in stable SD particles [*Potter and Stephenson*, 1986]. It can be used to estimate the anisotropy of such particles.

5. Methods Based on Measurements in High Fields

5.1. High Field Torque Magnetometer

[38] Because torque is easier to measure than magnetization, this method was initially used to determine the magnetic properties of crystals and compounds [*Townsend*, 1916; *Bozorth*, 1936; *Tarasov and Bitter*, 1937; *Williams*, 1937; *Tarasov*, 1939].

[39] The initial studies of torque magnetometry in natural samples assumed the anisotropy to be carried only by the ferromagnetic minerals [e.g., *King and Rees*, 1966; *Collinson et al.*, 1967; *Stone*, 1967; *Bhathal*, 1971; *Rees and Woodall*, 1975; *Folami and Hailwood*, 1991]. *Parma* [1988] designed a medium field magnetometer with fields ranging from 0 to 0.8 T that was used initially to evaluate the susceptibility of ferromagnetic phases above saturation and it has been proposed to separate theoretically the anisotropy components using the auxiliary energy density parameter [*Hrouda and Jelinek*, 1990]. *Bergmüller et al.* [1994] designed an instrument that uses a maximum field of 1.85 T and it has been also used to calculate the high-field susceptibility above the saturation of the ferromagnetic minerals [*Bergmüller and Heller*, 1996] or the paramagnetic energy density anisotropy [*Aubourg et al.*, 1995].

[40] The torsion exerted by a sample in an applied magnetic field is a fundamental definition in physics is

$$\mathbf{T} = \mathbf{m} \times \mathbf{B} \tag{9}$$

where **T** is the torque, **m** is the magnetization and **B** the applied field. Figure 7a shows the torque curve as a function of angle for several applied fields; the torque has a 2θ periodicity and increases with increasing applied field.

[41] When the magnetization is proportional to the applied field (paramagnetic or diamagnetic materials) the torque is proportional to the square of the applied field. *Porath and Chamalaun* [1966] proposed a model of torque proportional to field for intermediate fields in hematite which can also be extended to other minerals displaying crystalline anisotropy, e.g., pyrrhotite. Figure 7b shows the dependency of the amplitude with the applied field and the best fit theoretical curve above the saturation of the ferrimagnetic minerals for a peridotite sample. The absence of a linear dependency with field demonstrates that no hematite (or pyrrhotite) contributes to the torque signal.

[42] The different behavior of torque with applied field has been used to decompose the torque signal into the response for the three types of magnetic phases and compute the magnetic anisotropy ellipsoids [*Martín-Hernández and Hirt*, 2001, 2004]. *Hrouda and Jelinek* [1990] proposed a separation of magnetic anisotropy components based on the assumption that above the saturation of the ferrimagnetic components, the subtraction of two measurements using two different saturating fields is related with the paramagnetic minerals. Diamagnetism can be neglected, but in case it is not, the anisotropy of the diamagnetic subfabric is computed together with the paramagnetic ellipsoid. For one applied field, a new variable termed energy density tensor (**g**) is introduced and it has a different expression for paramagnetic and ferrimagnetic minerals [*Jelinek*, 1985, 1988].

$$\mathbf{g} = \frac{1}{2}\mu_0^{-1} B^2 \mathbf{l} \tag{10}$$

for paramagnetic minerals and

$$\mathbf{g} = \frac{1}{2} m_0 M_S^2 V_E \left(\mathbf{N_E} - \frac{1}{3}\mathbf{l} \right) \tag{11}$$

for ferrimagnetic minerals, where μ_o is the magnetic permeability of free space, B is the applied field, **l** is the deviatoric component of the susceptibility tensor, i.e., the tensor resulting for the substraction of the original tensor minus the mean value of the trace, M_S is the saturation magnetization of ferromagnetic grains, VE is the sum of the volumes of saturated grains and $\mathbf{N_E}$ is the tensor of demagnetization factor for the ferromagnetic grains [*Coe*, 1966].

[43] The low-field AMS usually agrees with the ferrimagnetic anisotropy principal directions because at low fields those minerals dominate the signal (Figure 7c). The paramagnetic anisotropy does not necessarily have to be subparallel to the low-field AMS (Figure 7d).

5.2. Cryogenic Magnetometer

[44] *Rochette et al.* [1983] proposed the use of magnetization as a function of different field and temperatures in order to identify the contributors to the magnetic anisotropy. *Rochette and Fillion* [1988] effectively calculated the differences between maximum and minimum susceptibility of paramagnetic and ferrimagnetic minerals. They used a cryogenic magnetometer with a variable field (0–4 T) and variable temperature (2–400 K) to separate the anisotropy of magnetic susceptibility due to ferromagnetic iron oxides and sulfides from that due to paramagnetic silicates. In high field ($H > 1$ T), the ferromagnetic component to the

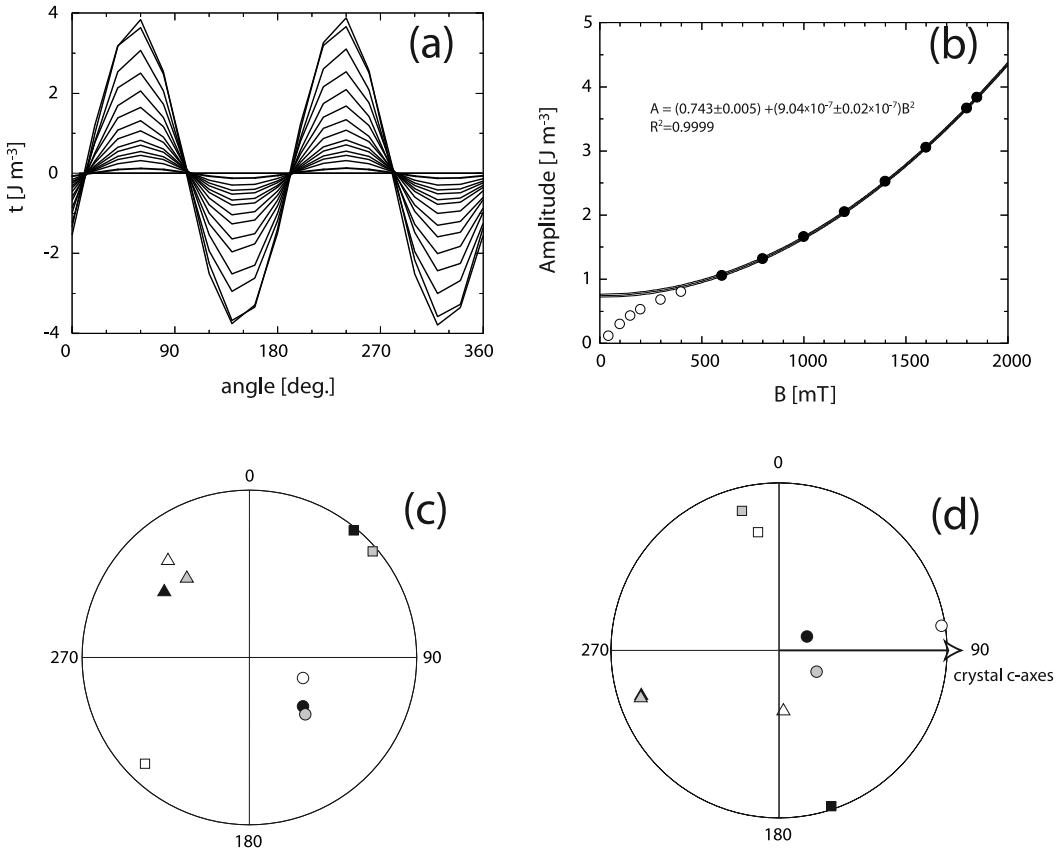

Figure 7. Torque procedure and measurements in a peridotite sample from the Ronda peridotites, Southern Spain and a chlorite single crystal. (a) Torque per unit volume as a function of angle in a peridotite sample. The torque has been measured at several applied fields ranging from 45 mT to 1850 mT. (b) Amplitude of the torque signal as a function of applied field for sample shown in Figure 7a. Open symbols represent amplitudes below the saturation of the ferromagnetic minerals, solid symbols represent amplitudes above the saturation of the ferromagnetic minerals. These values have been fitted into a second-order polynomial with only dependency on the square of the applied field. (c) Principal directions of the low-field AMS (solid symbols), anisotropy of the ferrimagnetic minerals evaluated above their saturation (gray symbols), and paramagnetic anisotropy of magnetic susceptibility (open symbols) for a peridotite sample. (d) Principal directions of anisotropy (same legend used in Figure 7c)) for a chlorite single crystal. The crystal basal plane is perpendicular to the horizontal plane; crystal c axis is parallel to the 90° declination axes.

anisotropy is generally saturated and magnetization is linear, defining the high-field magnetic susceptibility (χ_{HF}). The sample is rotated about three perpendicular axes and, considering variations of magnetization above the saturation of ferrimagnetic minerals to be due to the paramagnetic phases, the paramagnetic ellipsoid is computed. The magnetometer also allows measurements at different temperatures, therefore it is possible to distinguish between paramagnetic and diamagnetic fractions to the AMS. The same instrument and approach has been used to calculate the degree of anisotropy in weakly deformed black shales [*Aubourg et al.*, 1995]. This method is limited by the instrument to cubic samples of less than 10 mm.

5.3. Vibrating Sample Magnetometer

[45] The idea of using hysteresis loops to evaluate the paramagnetic/diamagnetic fabric in natural samples was proposed by *Borradaile and Werner* [1994] and by *Richter and van der Pluijm* [1994]. Years later, the general methodology for measurement of the high-field anisotropy of magnetic susceptibility (HFAMS) using a vibrating sample magnetometer has been described by *Thill et al.* [2000], *Ferré et al.* [2000] and *Kelso et al.* [2002]. The original method has been modified by *Ferré et al.* [2004] by (1) measuring cubic specimens, (2) normalizing results to saturation magnetization (*M*s) assumed to be insensitive to directional measurements, and (3) not using a bottom sample holder to allow frictionless motion of the sample. A series of hysteresis curves are acquired in different orientations for each specimen, using a vibrating sample magnetometer (Princeton VSM). Specimens are left lying on the VSM bench for at least 30 min before measurement to ensure thermal equilibrium with the pole gap space (19°C), which is cooler than the room temperature (21°C). The same sample holder is used for the directional measurements of the cubic specimens. The sample holder magnetic contribution is systematically subtracted in high-field calculations. Only

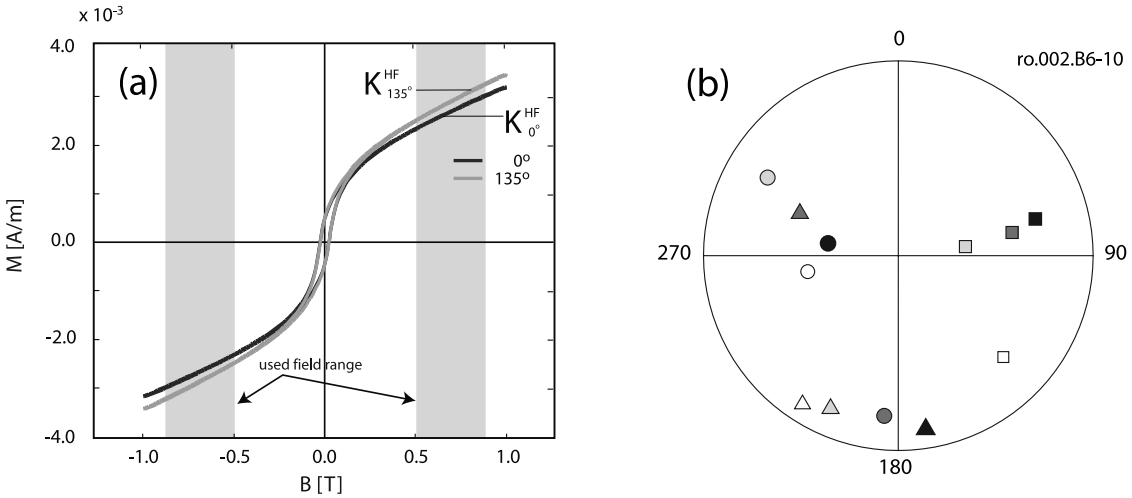

Figure 8. High-field separation of paramagnetic and ferromagnetic anisotropies in a peridotite sample from the Ronda massif, Spain. (a) High-field hysteresis loops in two positions. The high-field paramagnetic susceptibility has a 10% difference between position 1 and position 2. (b) Principal directions of the AMS where solid symbols represent the low-field AMS ellipsoid, open symbols represent the HF-AMS derived from hysteresis loops, dark gray symbols represent the ferrimagnetic ellipsoid measured in a high-field torque magnetometer, and light gray represent the paramagnetic ellipsoid derived by high-field torque magnetometry.

perfectly cubic specimens of 17 × 17 × 17 ± 0.2 mm are analyzed. The multiple positions are achieved by 15 rotation increments of 45° about the 3 perpendicular axes perpendicular to faces. Rotations were clockwise viewed from the top. This yields 24 hysteresis curves per specimen (about 1 min per curve). Symmetrical positions within the HFAMS measurement scheme are used to estimate the analytical error. Space for the specimen is provided by moving the pole pieces further apart (50 mm), which reduces the intensity of the field. The total measurement time per sample is approximately 22 min.

[46] The calculation of the high-field magnetic susceptibility is based on the measurement of the high-field slope (χ_{HF}) of the hysteresis curve. This is done by using the highest 15% of the hysteresis curve above magnetic saturation (Ms) (Figure 8a). The linear correlation coefficient was better than 0.9999 in all cases which shows that the considered segments were above magnetic saturation. Instrument artifacts, such as hooks on the terminations of hysteresis curves related to pole piece saturation, were removed before calculation. All specimens were run at a field of 0.9 T, which was sufficient to saturate all ferrimagnetic, grains in most specimens. Figure 8a illustrates hysteresis loops acquired for different orientations of a sample displaying both paramagnetic and ferromagnetic contributions.

[47] The response of the VSM instrument depends on the position of the magnetic dipoles with respect to the pick-up coils and therefore is sensitive to the specimen shape. The advantage of using cubic specimens is clear when considering that such specimens produce an unambiguous geometric/instrument response effect characterized by a 4ω periodicity, and that the instrument response is the same for all three axes, which is not the case with cylindrical specimens. This approach corrects for most variations due to the instrument response of the VSM but not for the fact that the magnetic center of the specimen (determined by optimizing the position of the specimen in between the coils) does not necessarily coincide with the geometric center of the specimen. This is the case when magnetic grains are nonuniformly oriented in the specimen. In addition to previous corrections, the high-field slope is finally normalized by dividing χ_{HF} by Ms, the saturation magnetization Ms can be assumed to be a constant (i.e., independent of measurement direction) for each specimen, and the normalization thus compensates for angular variations due to the sample shape and the instrument response function. The stereonet of Figure 8b shows a comparison of high-field AMS data with low-field AMS data and ferrimagnetic fabric only for peridotite samples from Ronda, Spain.

6. Other Methods

6.1. Methods Using Frequency Dependency

[48] A number of ferromagnetic (in the broad sense) minerals, such as magnetite, maghemite, and pyrrhotite exhibit frequency dependence in initial magnetic susceptibility [e.g., *Vincenz*, 1965; *Bathal*, 1971; *Dekkers*, 1988; *Worm et al.*, 1993]. This effect, referred to as electromagnetic susceptibility by *Ellwood et al.* [1993], is visible when the magnetic susceptibility is measured, in alternating field, by the electrical current induced in the solenoid of a susceptibility bridge. The complex apparent magnetic susceptibility is

$$k' + ik'' = \frac{3\mu(\sinh\alpha - \alpha\cosh\alpha) + 3/4\mu_o(\sinh\alpha - \alpha\cosh\alpha + \alpha^2\sinh\alpha)}{\mu(\sinh\alpha - \alpha\cosh\alpha) - \mu_o(\sinh\alpha - \alpha\cosh\alpha + \alpha^2\sinh\alpha)} \tag{12}$$

with k' as in-phase component, k'' as quadrature component, i imaginary number, $\alpha = r\,(i\mu\sigma\omega)^{1/2}$, r radius of the particles of conductive material in the specimen, μ as magnetic permeability, σ as electrical conductivity, ω as angular frequency of the applied field [*Worm et al.*, 1993].

[49] The in-phase component of the apparent susceptibility (k') decreases substantially above a certain frequency which depends on temperature, grain size and conductivity, for pyrrhotite is found to be 10 kHz [e.g., *Worm et al.*, 1993]. The quadrature component (k'') increases notably above 10 kHz in pyrrhotite and above 100 kHz in magnetite. Skin depth effects, related to the tendency for electric currents to flow near the surface of materials due to attenuation with depth, are practically negligible below 10 kHz.

[50] *Ellwood et al.* [1993] successfully isolated frequency-dependent AMS using synthetic specimens. This approach requires measurements to be performed at two frequencies (separated by about 2 orders of magnitude, e.g., 1 and 100 kHz) to unambiguously characterize frequency dependence. The new MFK1-FA,FB Kappabridge instruments offer the possibility of AMS measurement at three different frequencies of 976, 3904, and 15,616 Hz.

6.2. Statistical Methods

[51] *Henry* [1983] and *Henry and Daly* [1983] proposed a statistical method for separation of anisotropy based on the analysis of several specimens from the same site for the discrimination between the paramagnetic and ferromagnetic subfabric. The method assumes that under homogeneous strains, variations in the low-field AMS are due to local variations in the orientation or content of the ferromagnetic component. The paramagnetic fabric, attributed to the rock matrix is supposed to be equal for samples very close together. The individual low-field magnetic susceptibility semiaxes are expressed as a linear combination of the mean susceptibility and a constant term [*Henry and Daly*, 1983]. The low-field AMS semiaxes K_{ij} are expressed as

$$\overline{K} = p\overline{F} + (1-p)\overline{M} \tag{13}$$

where p is the ferromagnetic content in the sample, F_{ij} are the terms of the ferromagnetic susceptibility tensor and M_{ij} the terms of the matrix susceptibility.

[52] A similar relationship between low-field susceptibility, ferromagnetic and matrix susceptibility can also be written for the bulk properties:

$$\overline{K} = p\overline{F} + (1-p)\overline{M} \tag{14}$$

where $\overline{K}$ is the low-field bulk susceptibility, $\overline{F}$ is the low-field ferromagnetic bulk susceptibility and $\overline{M}$ is the matrix bulk susceptibility.

[53] The terms of the ferromagnetic fabric and the matrix fabric can be computed if the ferromagnetic low-field bulk susceptibility ($\overline{K}$) and the matrix bulk susceptibility ($\overline{M}$) are known. *Henry and Daly* [1983] and *Henry* [1983] proposed physical or chemical separation of the individual minerals. The auxiliary matrixes A_{ij} and B_{ij} are computed as the slope and the ordinate of the linear regression between the low-field susceptibility matrix terms (K_{ij}) and the low-field bulk susceptibility ($\overline{K}$), respectively.

[54] The susceptibility tensors are therefore derived as

$$\begin{aligned} F_{ij} &= A_{ij}\overline{F} + B_{ij} \\ M_{ij} &= A_{ij}\overline{M} + B_{ij} \end{aligned} \tag{15}$$

Henry and Daly [1983] applied the technique to a series of gneisses from the French Pyrenées and compared the results with the AIRM tensor determined on the same specimens. They showed a similar orientation of the ferromagnetic tensor derived by statistical method with respect to the AIRM principal directions. The method was successfully used to uncouple several deformations on Dalradian series from the southwest Scottish Highlands [*Henry*, 1985] and the Egletons granite in France [*Henry*, 1988]. However, this method is also known to lead to severe inconsistencies [*Jackson et al.*, 1991].

[55] *Constable and Tauxe* [1990] introduced the bootstrapping method applied to AMS tensors. On the basis of standard bootstrapping methods for unit vectors, AMS parametric bootstrapping can be performed: (1) sample parametric bootstrap and (2) site parametric bootstrap. This Monte Carlo approach can be considered a statistical separation of magnetic subfabrics following Henry's rationale if two requisites are fulfilled: (1) the paramagnetic and ferromagnetic fabrics are not subparallel and (2) there is a difference in the ferromagnetic content. The mean value obtained from the total bootstrapped tensor can be considered the dominant subfabric. The method has been extended since the appearance of a full software package for the analysis [*Tauxe*, 1998]. It has been successfully applied to evaluate the mean AMS fabric lava flows [*Cañón-Tapia et al.*, 1994], flow directions in dikes [*Constable and Tauxe*, 1990; *Tauxe et al.*, 1998], lineation in plutonic bodies [*Henry*, 1997; *Trindade et al.*, 2001b], mylonites [*Bascou et al.*, 2002] and phyllosilicate fabric in mudstones, shales and slates [*Parés and van der Pluijm*, 2002a, 2003].

[56] On the basis of the comparison between normalized AMS tensors by the mean susceptibility κ and the non-standardized AMS, the presence of multiple petrofabrics can be detected [*Borradaile*, 2001, 2003; *Borradaile and Jackson*, 2004].

7. Summary

[57] The anisotropy of magnetic susceptibility (AMS) has been extensively used for decades to constrain the orientation of minerals in rocks. The ferrimagnetic anisotropy generally originates from both magnetostatic (shape) and distribution (interaction) anisotropy of ferrimagnetic minerals. By contrast, paramagnetic anisotropy results mostly from magnetocrystalline (lattice preferred orientation) anisotropy. Therefore the significance of ferrimagnetic and paramagnetic anisotropy is clearly different. The success of the AMS method is due mainly to the rapid and reproducible nature of measurements. The interpretation of AMS in terms of deformation history is generally complicated by the fact that several phases contribute to the AMS tensor. Hence the separation of individual phase contribution to the AMS becomes necessary.

[58] The various approaches that have been used to characterize magnetic subfabrics are fundamentally differ-

ent in instrumental requirements and outputs. Table 1 summarizes the main advantages and inconveniences of the most commonly used separation techniques.

[59] Methods using the variation of paramagnetic susceptibility with temperature (from room temperature to low temperatures) can be useful providing that the specimen temperature is accurately known. Methods using the low-field AMS of heated rocks should be analyze carefully, the newly grown ferromagnetic minerals do not always mimic any preexisting structural feature. Remanence anisotropy tensors should not be subtracted from low-field AMS tensors because the two tensors represent physical properties that are not proportional to each other. High-field methods are suitable for magnetite/titanomagnetite bearing rocks, but accurate rock magnetic experiments are needed in order to guarantee the absence of high-coercivity fractions (pyrrhotite and/or hematite).

Appendix A: Separation of Diamagnetic Anisotropy

[60] Because of the atomic nature of the diamagnetism, all materials experience diamagnetic behavior when a magnetic field is applied. However, in most cases it is hidden by higher intensity paramagnetism or ferromagnetism. There are several techniques to measure directly diamagnetic anisotropy in diamagnetic materials, such as magnetization curves, low-field AMS [*Hrouda*, 1986], high-field torque magnetometry [*Owens and Bamford*, 1976] or high-field oscillations [*Uyeda*, 1993; *Uyeda et al.*, 1993]. None of these techniques performed a real separation of diamagnetic anisotropy that is very difficult because diamagnetic minerals have the same dependency of magnetization with field as do paramagnetic minerals and their susceptibility is also constant with temperature like ferromagnetic minerals. An attempt to a real separation between paramagnetic and diamagnetic fraction in synthetic mixtures has been recently proposed by making use of torque measurements at two temperatures [*Schmidt et al.*, 2007]. The method requires the a priori knowledge of the ration between low- and high-temperature paramagnetic susceptibility.

[61] The AMS of diamagnetic materials can be computed from a mathematical point of view. Some authors have subtracted the low-field diamagnetic anisotropy from the bulk low-field anisotropy by knowing the diamagnetic content and the diamagnetic single-crystal properties [*Hrouda*, 1986; *Schmidt et al.*, 2007]. If ferromagnetic minerals contribute significantly to the low-field AMS, it has been proposed to use the anisotropy of remanence to estimate the contribution for the total separation of AMS components [*Hrouda et al.*, 2000]. An alternative comes using the orientation of the diamagnetic minerals measuring its mineral fabric and compute the synthetic AMS of the diamagnetic minerals [*Owens and Rutter*, 1978; *de Wall et al.*, 2000].

[62] **Acknowledgments.** This research was supported by an EU Marie Curie Fellowship to F.M.H. (project MEIF-CT-2003-502133) and National Science Foundation to E.C.F. under grants EAR-0337458 and EAR-0521558. Sincere thanks to David Stone and Mike Jackson, who kindly reviewed a draft of this manuscript, and to Alicia Stanfill, who proofread the manuscript. The paper has also benefited by the comments from anonymous reviewers and Editor R. Enkin. Christine Franke provided valuable references.

References

Aubourg, C., and P. Robion (2002), Composite ferromagnetic fabrics (magnetite, greigite) measured by AMS and partial AARM in weakly strained sandstones from western Makran, Iran, *Geophys. J. Int.*, *151*, 729–737.

Aubourg, C., P. Rochette, and F. Bergmüller (1995), Composite magnetic fabric in weakly deformed black shales, *Phys. Earth Planet. Inter.*, *87*, 267–278.

Ballet, O., and J. M. D. Coey (1982), Magnetic properites of sheet silicates; 2:1 layer minerals, *Phys. Chem. Miner.*, *8*, 218–229.

Bascou, J., M. I. B. Raposo, A. Vauchez, and M. Egydio-Silva (2002), Titanohematite lattice-preferred orientation and magnetic anisotropy in high-temperature mylonites, *Earth Planet. Sci. Lett.*, *198*, 77–92.

Bathal, R. S. (1971), Magnetic anisotropy in rocks, *Earth Sci. Rev.*, *7*, 227–253.

Beausoleil, N., Lavallee, A. Yelon, O. Ballet, and J. M. D. Coey (1983), Magnetic properties of biotite micas, *J. Appl. Phys.*, *54*, 906–915.

Bergmüller, F., and F. Heller (1996), The field dependence of magnetic anisotropy parameters derived from high-field torque measurements, *Phys. Earth Planet. Inter.*, *96*, 61–76.

Bergmüller, F., C. Bärlocher, B. Geyer, M. Grieder, F. Heller, and P. Zweifel (1994), A torque magnetometer for measurements of the high-field anisotropy of rocks and crystals, *Meas. Sci. Technol.*, *5*, 1466–1470.

Bhathal, R. S. (1971), Magnetic anisotropy in rocks, *Earth Sci. Rev.*, *7*, 227–253.

Borradaile, G. (2001), Magnetic fabrics and petrofabrics: Their orientation distributions and anisotropies, *J. Struct. Geol.*, *23*, 1581–1593.

Borradaile, G. J. (2003), *Statistics or Earth Science Data, Space and Orientation*, 351 pp., Springer, New York.

Borradaile, G. J., and J. F. Dehls (1993), Regional kinematics inferred from magnetic subfabrics in Archean rocks of the northern Ontario, Canada, *J. Struct. Geol.*, *15*, 887–894.

Borradaile, G. J., and B. Henry (1997), Tectonic applications of magnetic susceptibility and its anisotropy, *Earth Sci. Rev.*, *42*, 49–93.

Borradaile, G. J., and M. Jackson (2004), Anisotropy of magnetic susceptibility (AMS): Magnetic petrofabrics of deformed rocks, in *Magnetic Fabric: Methods and Applications*, edited by F. Martin-Hernandez et al., *Geol. Soc. Spec. Publ.*, *238*, 299–360.

Borradaile, G. J., and F. Lagroix (2001), Magnetic fabrics reveal upper mantle flow fabrics in the Troodos Ophiolite Complex, Cyprus, *J. Struct. Geol.*, *23*, 1299–1317.

Borradaile, G. J., and M. Stupavsky (1995), Anisotropy of magnetic susceptibility: Measurement schemes, *Geophys. Res. Lett.*, *22*, 1957–1960.

Borradaile, G. J., and T. Werner (1994), Magnetic anisotropy of some phyllosilicates, *Tectonophysics*, *235*, 223–248.

Bozorth, R. M. (1936), Determination of ferromagnetic anisotropy in single crystals and in polycrystalline sheets, *Phys. Rev.*, *50*, 1076–1081.

Cagnoli, B., and D. Tarling (1997), The reliability of anisotropy of magnetic susceptibility (AMS) data as flow direction indicators in friable base surge and ignimbrite deposits: Italian examples, *J. Volcanol. Geotherm. Res.*, *75*, 309–320.

Cañón-Tapia, E. (2001), Factors affecting the relative importance of shape and distribution anisotropy in rocks: Theory and experiments, *Tectonophysics*, *340*, 117–131.

Cañón-Tapia, E., G. P. L. Walker, and E. Herrero-Bervera (1994), Magnetic fabric and flow direction in basaltic pahoehoe lava of Xitle volcano, Mexico, *J. Volcanol. Geotherm. Res.*, *65*, 249–263.

Clark, T. M., and B. J. Evans (1997), Influence of chemical composition on the crystalline morphologies of magnetite, *IEEE Trans. Magnet.*, *33*, 4257–4259.

Coe, R. S. (1966), Analysis of magnetic shape anisotropy using second rank tensors, *J. Geophys. Res.*, *71*, 2637–2644.

Collinson, D. W., K. M. Creer, and S. K. Runcorn (1967), *Methods in Palaeomagnetism*, 609 pp., Elsevier, New York.

Collombat, H., P. Rochette, and D. V. Kent (1993), Detection and correction of inclination shallowing in deep-sea sediments using the anisotropy of anhysteretic remanence, *Bull. Soc. Geol. Fr.*, *164*, 103–111.

Constable, C., and L. Tauxe (1990), The bootstrap for magnetic susceptibility tensors, *J. Geophys. Res.*, *95*, 8383–8395.

Cox, A., and R. R. Doell (1967), Measurement of high-coercivity anisotropy, in *Methods in Palaeomagnetism*, edited by D. W. Collinson, K. M. Creer, and S. K. Runcorn, pp. 477–482, Elsevier, New York.

Daly, L., and H. Zinsser (1973), Étude comparative des anisotropies de susceptibilité et d'aimantation rémanente isotherme: Conséquences pour l'analyse structurale et le paléomagnétisme, *Ann. Geophys.*, *29*, 189–200.

Dankers, P. H. M., and J. D. A. Zijderveld (1981), Alternating field demagnetization of rocks, and the problem of gyromagnetic remanence, *Earth Planet. Sci. Lett.*, *53*, 89–92.

Dean, B., R. W. Chantrell, A. Hart, D. A. Parker, and A. Stephenson (1990), The mathematical modeling of the acquisition of gyroremanent magnetization in a single domain particle, *J. Appl. Phys.*, *67*, 4481–4483.

Debacker, T. N., P. Robion, and M. Sintubin (2004), The anisotropy of magnetic susceptibility (AMS) in low-grade, cleaved pelitic rocks: Influence of cleavage/bedding angle and type and relative orientation of magnetic carriers, in *Magnetic Fabric: Methods and Applications*, edited by F. Martin-Hernandez et al., *Geol. Soc. Spec. Publ.*, *238*, 77–107.

de Boer, C. B., T. A. T. Mullender, and M. J. Dekkers (2001), Low-temperature behaviour of haematite: Susceptibility and magnetization increase on cycling through the Morin transition, *Geophys. J. Int.*, *146*, 201–216.

Dekkers, M. J. (1988), Magnetic properties of natural pyrrhotite. Part I: Behaviour of initial susceptibility and saturation-magnetization-related rock-magnetic parameters in a grain-size dependent framework, *Phys. Earth Planet. Inter.*, *52*, 376–393.

de Wall, H., M. Bestmann, and K. Ullemeyer (2000), Anisotropy of diamagnetic susceptibility in Tassos marble: A comparison between measured and modeled and modeled data, *J. Struct. Geol.*, *22*, 1761–1771.

Dunlop, D. J., and Ö. Özdemir (1997), *Rock Magnetism*, 573 pp., Cambridge Univ. Press, New York.

Edwards, J. (1984), Partial anhysteretic remanent magnetization produced in rotating samples, and comparison with corresponding rotational remanent magnetization, *Geophys. J. R. Astron. Soc.*, *77*, 619–637.

Ellwood, B. B., G. E. Terrell, and W. J. Cook (1993), Frequency dependence and the electromagnetic susceptibility tensor in magnetic fabric studies, *Phys. Earth Planet. Inter.*, *80*, 65–74.

Ferré, E. C., J. W. Thill, E. S. G. Rainey, and C. Teyssier (2000), Ductile flow in migmatites deduced from combined low- and high-field AMS measurements, *Eos Trans AGU*, *81*, 367.

Ferré, E. C., C. Bordarier, and J. S. Marsh (2002), Magma flow inferred from AMS fabrics in a layered mafic sill, Insizwa, South Africa, *Tectonophysics*, *354*, 1–23.

Ferré, E. C., F. Martín-Hernández, C. Teyssier, and M. Jackson (2004), Paramagnetic and ferromagnetic AMS in migmatites: Measurements in high and low fields and kinematic implications, *Geophys. J. Int.*, *157*, 1119–1129.

Ferré, E. C., B. Tikoff, and M. Jackson (2005), The magnetic anisotropy of mantle peridotites: Example from the Twin Sisters dunite, Washington, *Tectonophysics*, *398*, 141-166.

Flinn, D. (1956), On the development of the Funzie conglomerate, Fetlar, Shetland, *Scot. J. Geol.*, *64*, 480–505.

Folami, S. L., and E. A. Hailwood (1991), Magnetic fabric results from DSDP Hole 380a (Black Sea) and Hole 524 (South Atlantic) sediment cores: A case study for the comparison between low- and high-field torque magnetometer measurements, *Mar. Geophys. Res.*, *13*, 239–253.

Girdler, R. W. (1961), The measurement and computation of anisotropy of magnetic susceptibility in rocks, *Geophys. J. R. Astron. Soc.*, *5*, 34–44.

Graham, J. W. (1954), Magnetic susceptibility anisotropy, an unexploited petrofabric element, *Geol. Soc. Am. Bull.*, *65*, 1257–1258.

Granar, L. (1958), Magnetic measurements on Swedish varved sediments, *Ark. Geophys.*, *3*, 1–40.

Gregoire, V., M. de Saint Blanquat, A. Nedelec, and J.-L. Bouchez (1995), Shape anisotropy versus magnetic interactions of magnetite grains: Experiments and application to AMS in granitic rocks, *Geophys. Res. Lett.*, *22*, 2765–2768.

Hargraves, R. B., D. Johnson, and C. Y. Chan (1991), Distribution anisotropy: The cause of AMS in igneous rocks?, *Geophys. Res. Lett.*, *18*, 2193–2196.

Hejda, P., V. Kropácek, E. Petrovsky, T. Zelinka, and J. Zatecky (1992), Some magnetic properties of synthetic and natural haematite of different grain size, *Phys. Earth Planet. Inter.*, *70*, 261–272.

Henry, B. (1983), Interprétation quantitative de l'anisotropie de susceptibilité magnétique, *Tectonophysics*, *91*, 165–177.

Henry, B. (1985), Magnetic fabrics and superimposed deformations: Example of Dalradian rocks from the southwest Highlands of Scotland, *Phys. Earth Planet. Inter.*, *40*, 187–200.

Henry, B. (1988), The magnetic fabrics of the Egletons granite (France): Separation and structural implications, *Phys. Earth Planet. Inter.*, *51*, 253–263.

Henry, B. (1997), The magnetic zone axis: A new element of magnetic fabric for the interpretation of the magnetic lineation, *Tectonophysics*, *271*, 325.

Henry, B., and L. Daly (1983), From qualitative to quantitative magnetic anisotropy analysis: The prospect of finite strain calibration, *Tectonophysics*, *98*, 327–336.

Henry, B., D. Jordanova, N. Jordanova, C. Souque, and P. Robion (2003), Anisotropy of magnetic susceptibility of heated rocks, *Tectonophysics*, *366*, 241–258.

Hirt, A. M., and A. U. Gehring (1991), Thermal alteration of the magnetic mineralogy in ferruginous rocks, *J. Geophys. Res.*, *96*, 9947–9953.

Hodych, J. P., S. Bijaksana, and R. Patzold (1999), Using magnetic anisotropy to correct for paleomagnetic inclination shallowing in some magnetite-bearing deep-sea turbidites and limestones, *Tectonophysics*, *307*, 191–205.

Hrouda, F. (1986), The effect of quartz on the magnetic anisotropy of quartzite, *Stud. Geophys. Geod.*, *30*, 39–45.

Hrouda, F. (2002), The use of the anisotropy of magnetic remanence in the resolution of the anisotropy of magnetic susceptibility into its ferromagnetic and paramagnetic components, *Tectonophysics*, *347*, 269–281.

Hrouda, F., and V. Jelinek (1990), Resolution of ferrimagnetic and paramagnetic anisotropies in rocks, using combined low-field and high-field measurements, *Geophys. J. Int.*, *103*, 75–84.

Hrouda, F., J. Hanák, and S. Jacko (1988), Parallel magnetic fabrics in metamorphic, granitoid, and sedimentary rocks of the Branisko and Cierna Hora Mountains (E. Slovakia) and their tectonometamorphic control, *Phys. Earth Planet. Inter.*, *51*, 271–289.

Hrouda, F., V. Jelinek, and K. Zapletal (1997), Refined technique for susceptibility resolution into ferromagnetic and paramagnetic components based on susceptibility temperature-variation measurement, *Geophys. J. Int.*, *129*, 715–719.

Hrouda, F., B. Henry, and G. Borradaile (2000), Limitations of tensor subtraction in isolating diamagnetic fabrics by magnetic anisotropy, *Tectonophysics*, *322*, 303–310.

Hu, S., E. Appel, V. Hoffmann, W. W. Schmahl, and S. Wang (1998), Gyromagnetic remanence acquired by greigite (Fe_3S_4) during static three-axis alternating field demagnetization, *Geophys. J. Int.*, *134*, 831–842.

Hu, S., A. Stephenson, and E. Appel (2002), A study of gyroremanent magnetisation (GRM) and rotational remanent magnetisation (RRM) carried by greigite from lake sediments, *Geophys. J. Int.*, *151*, 469–474.

Ihmlé, P. F., A. M. Hirt, W. Lowrie, and D. Dietrich (1989), Inverse magnetic fabric in deformed limestones of the Morcles nappe, Switzerland, *Geophys. Res. Lett.*, *16*, 1383–1386.

Jackson, M., W. Gruber, J. Marvin, and S. K. Banerjee (1988), Partial anhysteretic remanence and its anisotropy: Applications and grainsize-dependence, *Geophys. Res. Lett.*, *15*, 440–443.

Jackson, M. J. (1991), Anisotropy of magnetic remanence: A brief review of mineralogical sources, physical origins, and geological applications, and comparison with susceptibility anisotropy, *Pure Appl. Geophys.*, *136*, 1–28.

Jackson, M. J., and L. Tauxe (1991), Anisotropy of magnetic susceptibility and remanence: Developments in the characterization of tectonic, sedimentary, and igneous fabric, *U.S. Natl. Rep. Int. Union Geod. Geophys. 1987–1990*, *Rev. Geophys.*, *29*, 371–376.

Jackson, M. J., S. K. Banerjee, J. A. Marvin, R. Lu, and W. Gruber (1991), Detrital remanence, inclination errors, and anhysteretic remanence anisotropy: Quantitative model and experimental results, *Geophys. J. Int.*, *104*, 95–103.

Jelinek, V. (1981), Characterization of the magnetic fabric of rocks, *Tectonophysics*, *79*, T63–T67.

Jelinek, V. (1985), The physical principles of measuring magnetic anisotropy with the torque magnetometer, *Trav. Inst. Geophys. Acad. Tchecoslov. Sci.*, *608*, 177–198.

Jelinek, V. (1988), Potential energy density tensor and magnetic anisotropy problems, *Phys. Earth Planet. Inter.*, *51*, 361–364.

Jelinek, V. (1993), Theory and measurement of the anisotropy of isothermal remanent magnetization of rocks, *Trav. Geophys.*, *37*, 124–134.

Jover, O., P. Rochette, J. P. Lorand, M. Maeder, and J. L. Bouchez (1989), Magnetic mineralogy of some granites from the French Massif Central: Origin of their low-field susceptibility, *Phys. Earth Planet. Inter.*, *55*, 79–92.

Just, J., A. Kontny, H. de Wall, A. M. Hirt, and F. Martín-Hernández (2004), Development of magnetic fabrics during hydrothermal alteration in the Soultz-sous-Forêts granite from the EPS-1 drilling, Upper Rhine Graben, in *Magnetic Fabric: Methods and Applications*, edited by F. Martin-Hernandez et al., *Geol. Soc. Spec. Publ.*, *238*, 509–526.

Kelso, P. R., B. Tikoff, M. Jackson, and W. Sun (2002), A new method for the separation of paramagnetic and ferromagnetic susceptibility anisotropy using low field and high field methods, *Geophys. J. Int.*, *151*, 345–359.

Kim, B., and K. P. Kodama (2004), A compaction correction for the paleomagnetism of the Nanaimo Group sedimentary rocks: Implications for the Baja British Columbia hypothesis, *J. Geophys. Res.*, *109*, B02102, doi:10.1029/2003JB002696.

King, R. F., and A. I. Rees (1966), Detrital magnetism in sediments: An examination of some theoretical models, *J. Geophys. Res.*, *71*, 561–571.

Kodama, K. P. (1995), Magnetic fabrics, *U.S. Natl. Rep. Int. Union Geod. Geophys. 1991–1994*, *Rev. Geophys.*, *33*, 129–136.

Kodama, K. P., and M. J. Dekkers (2004), Magnetic anisotropy as an aid to identifying CRM and DRM in red sedimentary rocks, *Stud. Geophys. Geod.*, *48*, 747–766.

Kodama, K. P., and W.-W. Sun (1992), Magnetic anisotropy as a correction for compaction-caused paleomagnetic inclination shallowing, *Geophys. J. Int.*, *111*, 465–469.

Lagroix, F., and G. Borradaile (2000), Magnetic fabric interpretation complicated by inclusions in mafic silicates, *Tectonophysics*, *325*, 207–225.

Liu, J.-Z. (1986), Morin transition in hematite doped with iridium ions, *J. Magnet. Magn. Mater.*, *54–57*, 901–902.

Lu, G., and C. McCabe (1993), Magnetic fabric determined from ARM and IRM anisotropies in Paleozoic carbonates, southern Appalachian basin, *Geophys. Res. Lett.*, *20*, 1099–1102.

Lüneburg, C. M., S. A. Lampert, H. K. Lebit, A. M. Hirt, M. Casey, and W. Lowrie (1999), Magnetic anisotropy, rock fabrics and finite strain in deformed sediments of SW Sardinia (Italy), *Tectonophysics*, *307*, 51–74.

Martín-Hernández, F., and A. M. Hirt (2001), Separation of ferrimagnetic and paramagnetic anisotropies using a high-field torsion magnetometer, *Tectonophysics*, *337*, 209–221.

Martín-Hernández, F., and A. M. Hirt (2003), Paramagnetic anisotropy of magnetic susceptibility in biotite, muscovite and chlorite single crystals, *Tectonophysics*, *367*, 13–28.

Martín-Hernández, F., and A. M. Hirt (2004), A method for the separation of paramagnetic, ferrimagnetic and hematite magnetic subfabrics using high-field torque magnetometer, *Geophys. J. Int.*, *157*, 117–127.

McCabe, C., M. Jackson, and B. B. Ellwood (1985), Magnetic anisotropy in the Trenton limestone: Results of a new technique, anisotropy of anhysteretic susceptibility, *Geophys. Res. Lett.*, *12*, 333–336.

Mintsa Mi Guema, T., R. I. F. Trindade, J. L. Bouchez, and P. Launeau (2002), Selective thermal enhancement of magnetic fabrics from the Carnmenellis granite (British Cornwall), *Phys. Chem. Earth, Parts A/B/C*, *27*, 1281–1287.

Miranda, J. M., P. F. Silva, N. Loureno, B. Henry, R. Costa, and T. Saldanha Team (2002), Study of the Saldanha Massif (MAR, 36°34′N): Constraints from rock magnetic and geophysical data, *Mar. Geophys. Res.*, *23*, 299–318.

Morin, J. (1950), Magnetic susceptibility of α-Fe_2O_3 and Fe_2O_3 with added titanium, *Phys. Rev.*, *78*, 819–820.

Morrish, A. H. (1965), *The Physical Principles of Magnetism*, 680 pp., John Wiley, Hoboken, N. J.

Nagata, T. (1961), *Rock Magnetism*, 350 pp., Maruzen, Tokyo.

Nakamura, N., and G. Borradaile (2001), Strain, anisotropy of anhysteretic remanence, and anisotropy of magnetic susceptibility in a slaty tuff, *Phys. Earth Planet. Inter.*, *125*, 85–93.

Newman, J., W. M. Lamb, M. R. Drury, and R. L. M. Vissers (1999), Deformation processes in a peridotite shear zone: Reaction-softening by an H2O-deficient, continuous net transfer reaction, *Tectonophysics*, *303*, 193–222.

Owens, W. H., and D. Bamford (1976), Magnetic, seismic and other anisotropic properties of rock fabric, *Philos. Trans. R. Soc. London, Ser. A*, *283*, 55–68.

Owens, W. H., and E. H. Rutter (1978), The development of magnetic susceptibility anisotropy through crystallographic preferred orientation in a calcite rock, *Phys. Earth Planet. Inter.*, *16*, 215–222.

Parés, J. M., and B. A. van der Pluijm (2002a), Evaluating magnetic lineations (AMS) in deformed rocks, *Tectonophysics*, *350*, 283–298.

Parés, J. M., and B. A. van der Pluijm (2002b), Phyllosilicate fabric characterization by Low-Temperature Anisotropy of Magnetic Susceptibility (LT-AMS), *Geophys. Res. Lett.*, *29*(24), 2215, doi:10.1029/2002GL015459.

Parés, J. M., and B. A. van der Pluijm (2003), Magnetic fabrics and strain in pencil structures of the Knobs Formation, Valley and Ridge Province, US Appalachians, *J. Struct. Geol.*, *25*, 1349–1358.

Parma, J. (1988), An automated torque meter for rapid measurement of high field magnetic anisotropy of rocks, *Phys. Earth Planet. Inter.*, *51*, 387–389.

Porath, H., and F. H. Chamalaun (1966), The magnetic anisotropy of hematite bearing rocks, *Pure Appl. Geophys.*, *67*, 81–88.

Potter, D. K. (2004), A comparison of anisotropy of magnetic remanence methods - a user's guide for application to paleomagnetism and magnetic fabric studies, in *Magnetic Fabric: Methods and Applications*, edited by F. Martin-Hernandez et al., *Geol. Soc. Spec. Publ.*, *238*, 21–35.

Potter, D. K., and A. Stephenson (1986), The detection of fine particles of magnetite using anhysteretic and rotational remanent magnetization, *Geophys. J. R. Astron. Soc.*, *87*, 569–582.

Potter, D. K., and A. Stephenson (1990), Field-impressed anisotropies of magnetic susceptibility and remanence in minerals, *J. Geophys. Res.*, *95*, 15,573–15,588.

Raposo, M. I. B., and M. Egydio-Silva (2001), Magnetic fabric studies of high-grade metamorphic rocks from the Juiz de Fora Complex, Riberia Belt, southeastern Brazil, *Int. Geol. Rev.*, *43*, 441–456.

Raposo, M. I. B., A. O. Chaves, P. Lojkasek-Lima, M. S. D'Agrella, and W. Texeira (2004), Magnetic fabrics and rock magnetism of Proterozoic dike swarm from the southern Sao Francisco Craton, Minas Gerais State, Brazil, *Tectonophysics*, *378*, 43–63.

Rees, A. I., and W. A. Woodall (1975), The magnetic fabric of some laboratory-deposited sediments, *Earth Planet. Sci. Lett.*, *25*, 121–130.

Richter, C., and B. A. van der Pluijm (1994), Separation of paramagnetic and ferrimagnetic susceptibilities using low temperature magnetic susceptibilities and comparison with high field methods, *Phys. Earth Planet. Inter.*, *82*, 111–121.

Robion, P., O. Averbuch, and M. Sintubin (1999), Fabric development and metamorphic evolution of lower Palaeozoic slaty rocks from the Rocroi massif (French-Belgian Ardennes): New constraints from magnetic fabrics, phyllosilicate preferred orientation and illite crystallinity data, *Tectonophysics*, *309*, 257–273.

Rochette, P. (1988), Inverse magnetic fabric in carbonate-bearing rocks, *Earth Planet. Sci. Lett.*, *90*, 229–237.

Rochette, P., and G. Fillion (1988), Identification of multicomponent anisotropies in rocks using various field and temperature values in a cryogenic magnetometer, *Phys. Earth Planet. Inter.*, *51*, 379–386.

Rochette, P., G. Fillion, P. Mollard, and R. Vergne (1983), Utilisation d'un magnétomètre à effet Josephson pour l'analyse de l'anisotropie magnétique des roches, *C. R. Acad. Sci.*, *296*, 557–559.

Rochette, P., M. Jackson, and C. Aubourg (1992), Rock magnetism and the interpretation of anisotropy of magnetic susceptibility, *Rev. Geophys.*, *30*, 209–226.

Roperch, P., and G. K. Taylor (1986), The importance of gyromagnetic remanence in alternating field demagnetization; some new data and experiments on GRM and RRM, *Geophys. J. R. Astron. Soc.*, *87*, 949–965.

Sangode, S. J., and J. Bloemendal (2004), Pedogenic transformation of magnetic minerals in Pliocene-Pleistocene palaeosols of the Siwalik Group, NW Himalaya, India, *Palaeogeogr. Palaeoclimatol. Palaeoecol.*, *212*, 95–118.

Schmidbauer, E., and P. W. Readman (1982), Low temperature magnetic properties of Ti-rich Fe-Ti spinels, *J. Magnet. Magnet. Mater.*, *27*, 114–118.

Schmidt, V., A. M. Hirt, P. Rosselli, and F. Martin-Hernandez (2007), Separation of diamagnetic and paramagnetic anisotropy by high-field, low-temperature torque measurements, *Geophys. J. Int.*, *168*, 40–47, doi:10.1111/j.1365-246X.2006.03202.x.

Schultz-Krutisch, T., and F. Heller (1985), Measurement of magnetic susceptibility anisotropy in Buntsandstein deposits form southern Germany, *J. Geophys.*, *56*, 51–58.

Sizaret, S., Y. Chen, A. Chauvet, E. Marcoux, and J. C. Touray (2003), Magnetic fabrics and fluid flow directions in hydrothermal systems: A case study in the Chaillac Ba-F-Fe deposits (France), *Earth Planet. Sci. Lett.*, *206*, 555–570.

Smith, R. W., and M. Fuller (1967), Alpha-hematite: Stable remanence and memory, *Science*, *156*, 1130–1134.

Snowball, I. F. (1997a), The detection of single-domain greigite (Fe_3S_4) using rotational remanent magnetization (RRM) and the effective gyro field (Bg): Mineral magnetic and palaeomagnetic applications, *Geophys. J. Int.*, *130*, 704–716.

Snowball, I. F. (1997b), Gyroremanent magnetization and the magnetic properties of greigite-bearing clays in southern Sweden, *Geophys. J. Int.*, *129*, 624–636.

Stacey, F. D., and S. K. Banerjee (1974), *The Physical Principles of Rock Magnetism*, 195 pp., Elsevier, New York.

Stephenson, A. (1980a), Gyromagnetism and the remanence acquired by a rotating rock in an alternating field, *Nature*, *284*, 48–49.

Stephenson, A. (1980b), A gyroremanent magnetization in anisotropic magnetic material, *Nature*, *284*, 49–51.

Stephenson, A. (1980c), Rotational remanent magnetization and the torque exerted on a rotating rock in an alternating magnetic field, *Geophys. J. R. Astron. Soc.*, *62*, 113–132.

Stephenson, A. (1981a), Gyromagnetic remanence and anisotropy in single-domain particles, rocks, and magnetic recording tape, *Philos. Mag. B*, *44*, 635–664.

Stephenson, A. (1981b), Gyroremanent magnetization in a weakly anisotropic rock sample, *Phys. Earth Planet. Inter.*, *25*, 163–166.

Stephenson, A. (1994), Distribution anisotropy: Two simple models for magnetic lineation and foliation, *Phys. Earth Planet. Inter.*, *82*, 49–53.

Stephenson, A., and D. K. Potter (1987), Gyroremanent magnetizations in dilute anisotropic dispersions of gamma ferric oxide particles from magnetic recording tape, *IEEE Trans. Magnet.*, *MAG-23*, 3820–3830.

Stephenson, A., and I. F. Snowball (2001), A large gyromagnetic effect in greigite, *Geophys. J. Int.*, *145*, 570–575.

Stephenson, A., S. Sadikun, and D. K. Potter (1986), A theoretical and experimental comparison of the anisotropies of magnetic susceptibility and remanence in rocks and minerals, *Geophys. J. R. Astron. Soc.*, *84*, 185–200.

Stone, D. B. (1967), Torsion-balance method of measuring anisotropic susceptibility, in *Methods in Palaeomagnetism*, edited by D. W. Collinson, K. M. Creer, and S. K. Runcorn, pp. 381–386, Elsevier, New York.

Tan, X., and K. P. Kodama (2002), Magnetic anisotropy and paleomagnetic inclination shallowing in red beds: Evidence from the Mississippian Mauch Chunk Formation, Pennsylvania, *J. Geophys. Res.*, *107*(B11), 2311, doi:10.1029/2001JB001636.

Tan, X., K. P. Kodama, H. Chen, D. Fang, D. Sun, and Y. Li (2003), Paleomagnetism and magnetic anisotropy of Cretaceous red beds from the Tarim basin, northwest China: Evidence for a rock magnetic cause of anomalously shallow paleomagnetic inclinations from central Asia, *J. Geophys. Res.*, *108*(B2), 2107, doi:10.1029/2001JB001608.

Tarasov, L. P. (1939), Dependence of ferromagnetic anisotropy on the field strength, *Phys. Rev.*, *56*, 1224–1230.

Tarasov, L. P., and F. Bitter (1937), Precise magnetic torque measurements on single crystals of iron, *Phys. Rev.*, *52*, 353–360.

Tarling, D. H., and F. Hrouda (1993), *The Magnetic Anisotropy of Rocks*, 217 pp., CRC Press, Boca Raton, Fla.

Tauxe, L. (1998), *Paleomagnetic Principles and Practice*, 297 pp., Springer, New York.

Tauxe, L., C. G. Constable, L. Stokking, and C. Badgely (1990), Use of anisotropy to determine the origin of characteristic remanence in the Siwalik red beds of northern Pakistan, *J. Geophys. Res.*, *95*, 4391–4404.

Tauxe, L., J. S. Gee, and H. Staudigel (1998), Flow directions in dikes from anisotropy of magnetic susceptibility data: The bootstrap way, *J. Geophys. Res.*, *103*, 17,775–17,790.

Thill, J. W., E. C. Ferré, E. S. G. Rainey, and C. Teyssier (2000), Separation of AMS into ferrimagnetic and paramagnetic components in migmatites: A possible shear-sense indicator?, *Eos Trans. AGU*, *81*, 367.

Townsend, T. (1916), The magnetic properties of hematite, *Rev. Geophys.*, *8*, 721–737.

Trindade, R. I. F., J. L. Bouchez, O. Bolle, A. Nedelec, A. Peschler, and F. Poitrasson (2001a), Secondary fabrics revealed by remanence anisotropy: Methodological study and examples from plutonic rocks, *Geophys. J. Int.*, *147*, 310–318.

Trindade, R. I. F., T. Mintsa Mi Nguema, and J. L. Bouchez (2001b), Thermally enhanced mimetic fabric of magnetite in a biotite granite, *Geophys. Res. Lett.*, *28*, 2687–2690.

Uyeda, C. (1993), Diamagnetic anisotropies of oxide minerals, *Phys. Chem. Miner.*, *20*, 77–81.

Uyeda, C., T. Takeuchi, A. Yamagishi, A. Tsuchiyama, T. Yamanaka, and M. Date (1993), Diamagnetic anisotropy of sheet silicates, *Phys. Chem. Miner.*, *20*, 369–374.

Uyeda, S. (1958), Thermo-remanent magnetism as a medium of palaeomagnetism, with special reference to reverse thermo-remanent magnetism, *Jpn. J. Geophys.*, *2*, 1–123.

Vaughn, J., K. P. Kodama, and D. P. Smith (2005), Correction of inclination shallowing and its tectonic implications: The Cretaceous Perforada Formation, Baja California, *Earth Planet. Sci. Lett.*, *232*, 71–82.

Verwey, E. J. (1939), Electronic conduction of magnetite (Fe_3O_4) and its transition point at low temperature, *Nature*, *144*, 327–328.

Vincent, D., S. Neveu, L. Jorat, and G. Noyel (1996), Gyromagnetic resonance in ferrofluids made from manganese ferrite or magnetite particles: Influence of a constant axial magnetic field., *J. Magnet. Magnet. Mater.*, *163*, 216–220.

Vincenz, S. A. (1965), Frequency dependence of magnetic susceptibility of rocks in weak alternating fields, *J. Geophys. Res.*, *70*, 1371–1377.

Williams, H. J. (1937), Magnetic properties of single crystals of silicon iron, *Phys. Rev.*, *52*, 747–751.

Worm, H.-U., D. Clark, and M. J. Dekkers (1993), Magnetic susceptibility of pyrrhotite: Grain size, field and frequency dependence, *Geophys. J. Int.*, *114*, 127–137.

Zapletal, K. (1990), Low-field susceptibility anisotropy of some biotite crystals, *Phys. Earth Planet. Inter.*, *63*, 85–97.

F. Martín-Hernández, Paleomagnetic Laboratory Fort Hoofddijk, Faculty of Geosciences, Utrecht University, NL-3584 CD Utrecht, Netherlands. (fatima@geo.uu.nl)

E. C. Ferré, Department of Geology, Southern Illinois University, Carbondale, IL 62901-4324, USA. (eferre@geo.siu.edu)